Production of Functional Glucagon-Secreting α-Cells From Human Embryonic Stem Cells

Alireza Rezania,[1] Michael J. Riedel,[2] Rhonda D. Wideman,[2] Francis Karanu,[1] Ziliang Ao,[3] Garth L. Warnock,[3] and Timothy J. Kieffer[2,3]

OBJECTIVE—Differentiation of human embryonic stem (hES) cells to fully developed cell types holds great therapeutic promise. Despite significant progress, the conversion of hES cells to stable, fully differentiated endocrine cells that exhibit physiologically regulated hormone secretion has not yet been achieved. Here we describe an efficient differentiation protocol for the in vitro conversion of hES cells to functional glucagon-producing α-cells.

RESEARCH DESIGN AND METHODS—Using a combination of small molecule screening and empirical testing, we developed a six-stage differentiation protocol for creating functional α-cells. An extensive in vitro and in vivo characterization of the differentiated cells was performed.

RESULTS—A high rate of synaptophysin expression (>75%) and robust expression of glucagon and the α-cell transcription factor ARX was achieved. After a transient polyhormonal state in which cells coexpress glucagon and insulin, maturation in vitro or in vivo resulted in depletion of insulin and other β-cell markers with concomitant enrichment of α-cell markers. After transplantation, these cells secreted fully processed, biologically active glucagon in response to physiologic stimuli including prolonged fasting and amino acid challenge. Moreover, glucagon release from transplanted cells was sufficient to reduce demand for pancreatic glucagon, resulting in a significant decrease in pancreatic α-cell mass.

CONCLUSIONS—These results indicate that fully differentiated pancreatic endocrine cells can be created via stepwise differentiation of hES cells. These cells may serve as a useful screening tool for the identification of compounds that modulate glucagon secretion as well as those that promote the transdifferentiation of α-cells to β-cells. ***Diabetes*** **60:239–247, 2011**

Human embryonic stem (hES) cells hold great potential for the development of replacement therapies for conditions including heart disease, spinal cord injury, and diabetes. With the recent FDA approval of the first U.S.-based clinical trial for the use of cells derived from hES cells (1), there is renewed optimism that other stem cell–based therapies may soon be developed and tested clinically. Treatment of type 1 diabetes with cadaveric human islets has been promising, suggesting that a cell-based therapy for this disease may be possible given sufficient availability of transplant material. hES cells can be efficiently differentiated to definitive endoderm (2,3) and further to endocrine-like polyhormonal cells that are capable of hormone secretion in response to some physiologic and pharmacologic stimuli (4–6). However, the formation of mature, single hormone-expressing endocrine cells in culture remains a major hurdle. Recent efforts have been focused on the maturation of partially differentiated cells toward β-cells in vivo after transplantation into model animals (7,8); however, the clinical use of partially differentiated cells may present an unacceptable risk of tumor formation. We therefore sought to develop a protocol for the in vitro differentiation of a functional, terminally differentiated endocrine cell type from hES cells. In pursuing our goal of ultimately developing a scalable protocol to produce β-cells, we established a method to convert hES cells to functional glucagon-expressing cells that resemble mature pancreatic α-cells.

RESEARCH DESIGN AND METHODS

Differentiation of hES cells. The H1 hES cell line was obtained from WiCell Research Institute (Madison, WI), and cultured according to instructions provided by the source institute. Briefly, cells were cultured on 1:30 diluted, growth factor-reduced Matrigel- (Invitrogen; Carlsbad, CA) coated plates in mouse embryonic fibroblast (MEF)-conditioned media as previously described (9). When ~80% confluent (~5–7 days after plating), hES cells were treated with 1 mg/ml Dispase (Invitrogen) for 5 min and then gently scraped off the surface using a 5-ml pipette. Cells were spun at 900 rpm for 3 min, and the pellet was resuspended and replated at a 1:3 to 1:4 ratio of hES cells in MEF-conditioned media supplemented with 16 ng/ml of fibroblast growth factor 2 (FGF2) (R&D Systems; Minneapolis, MN). Details of stage-specific treatments are described in the supplementary data in the online appendix available at http://diabetes.diabetesjournals.org/cgi/content/full/db10-0573/DC1.

Human islets. Human islets were obtained from the Irving K. Barber Human Islet Isolation Laboratory (Vancouver, BC) and were maintained in Final Wash Media (Mediatech, Inc., Herndon, VA). For dithizone staining, islets were washed with PBS(-), then incubated in a filter-sterilized 78 μmol/l dithizone (Sigma-Aldrich) solution in DMSO for 1 h. Islets were then washed with Dulbecco's modified Eagle's medium/F12 media to remove excess dithizone and examined under a light microscope.

Quantitative RT-PCR. Total RNA was extracted with the RNeasy Mini Kit (Qiagen; Valencia, CA) and reverse-transcribed using the High Capacity cDNA Reverse Transcription Kit (Applied Biosystems, Foster City, CA) according to the manufacturer's instructions. The cDNA was amplified by PCR using Taqman Universal Master Mix and Taqman Gene Expression Assays (see supplementary Table 2), which were preloaded onto custom Taqman Arrays (Applied Biosystems). Data were analyzed using Sequence Detection Software (Applied Biosystems) and normalized to undifferentiated ES cells using the ΔΔCt method.

Insulin, glucagon, and DNA content. Cells were lysed by suspension in Tris-EDTA (pH 7.4) followed by sonication until cell membranes were dispersed. DNA content was determined using the Quant-IT Picogreen kit

From the [1]BetaLogics Venture, Centocor Research and Development, Skillman, New Jersey; the [2]Laboratory of Molecular and Cellular Medicine, Department of Cellular and Physiological Sciences, Life Sciences Institute, University of British Columbia, Vancouver, British Columbia, Canada; and the [3]Department of Surgery, University of British Columbia, Vancouver, British Columbia, Canada.

Corresponding author: Timothy J. Kieffer, tim.kieffer@ubc.ca.

Received 22 April 2010 and accepted 20 September 2010. Published ahead of print at http://diabetes.diabetesjournals.org on 22 October 2010. DOI: 10.2337/db10-0573.

A.R., M.J.R., and R.D.W. contributed equally to this work.

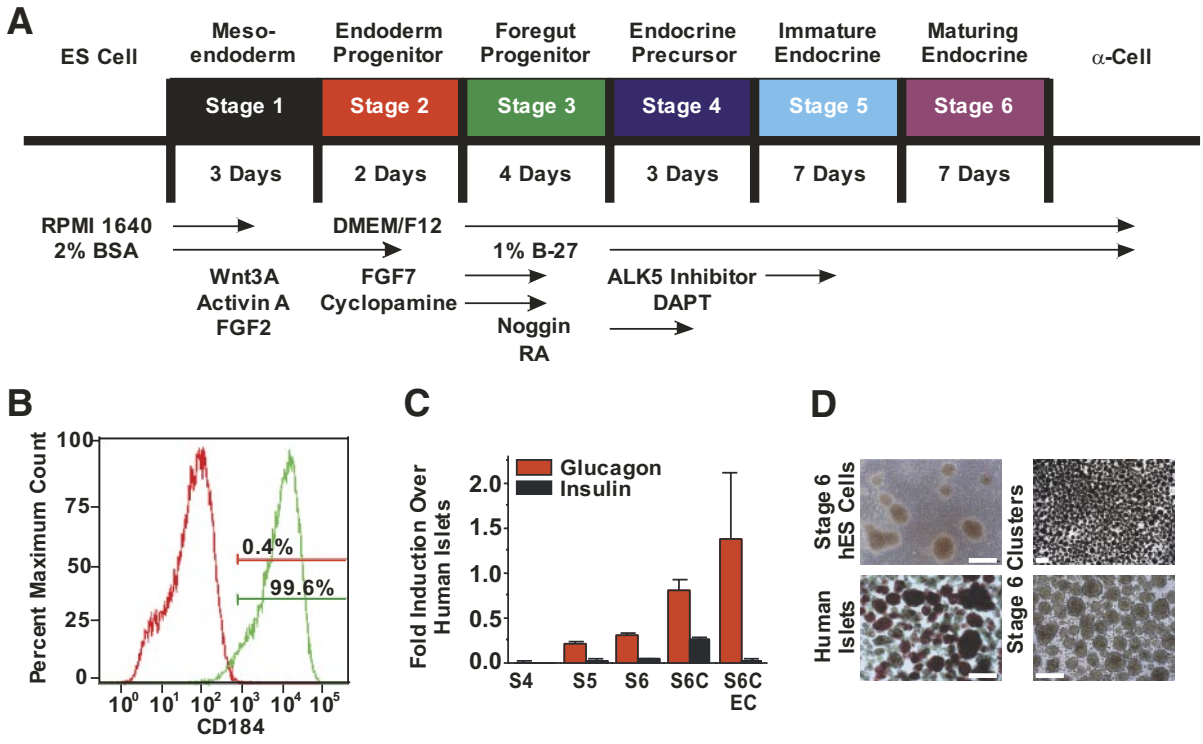

FIG. 1. Differentiation of hES cells to maturing endocrine cells. *A*: Schematic representation of 6-stage differentiation protocol, with media and supplements shown below. *B*: Representative fluorescence-activated cell sorter analysis of CD184 expression (*green line*) in hES cells at stage 1 of differentiation protocol; isotype control in *red*. Percentage values indicate number of cells expressing CD184 in each group. *C*: *GCG* and *INS* expression as measured by qRT-PCR in hES cells at stages 4–6, and in stage 6 clusters before (S6C) and after (S6C EC) an extended 4-week culture period. Data are expressed as fold induction versus human islet control; $n = 3$ for each stage of differentiation. Error bars indicate SE. *D*: Representative brightfield images of stage 6 hES cells, Stage 6 clusters, and dithizone-stained human islets. Scale bar, 150 μm. (A high-quality color representation of this figure is available in the online issue.)

(Invitrogen), whereas insulin and glucagon content were determined using Insulin and Glucagon ELISA, respectively (Alpco Diagnostics; Salem, NH).

Flow cytometry. Differentiated cells were released into single-cell suspensions by incubation in TrypLE Express (Invitrogen), fixed, and stained using antibodies directed against intracellular proteins as indicated in the text. A detailed description of staining can be found in the online supplementary data.

Immunocytochemistry. Isolated human islets and stage 6 differentiated hES cell clusters were fixed in 4% paraformaldehyde (PFA) overnight at 4°C, then embedded in a 1% agarose in PBS gel before being paraffin embedded and sectioned for immunostaining. Graft-bearing kidneys and pancreata were fixed in 4% PFA overnight at 4°C before being paraffin embedded and sectioned. All sections were cut at a thickness of 5 μm. Staining procedures and antibodies used are detailed in the online supplementary data.

α-Cell mass quantification. After DAB staining, pancreas sections were digitally rendered using a ScanScope CS digital slide scanner (Aperio Technologies, Vista, CA) and analyzed using the ImageScope positive pixel count, version 9 algorithm (Aperio Technologies).

Perifusion. Equal volumes of human islets or stage 6 hES cell–derived cells were loaded into temperature-/CO_2-controlled chambers of an Endotronics Acu-syst S Perifusion apparatus. HEPES-buffered Krebs Ringers Bicarbonate Buffer (KRBB) containing 0.5% BSA was pumped through the chambers at ~350 μl/min after a 1-h preincubation under basal conditions. Fractions were collected every 5 min and assayed for insulin and glucagon via radioimmunoassay (Millipore; Billerica, MA).

Animal studies and transplantation of hES cell–derived cells. All experiments were approved by the University of British Columbia Animal Care Committee. Male B6.129S7-Rag^{Tm1Mom}/J mice (stock 2,216) were obtained from the Jackson Laboratories (Bar Harbor, ME) at 8–10 weeks of age. Mice were maintained on a 12-h light/dark cycle and had ad libitum access to a standard irradiated diet (PicoLab 20; #5058l PMI International; St. Louis, MO). Blood glucose and body weight were monitored 2–3 times weekly after a 4-h morning fast. Blood glucose was measured via the saphenous vein using a handheld glucometer (Lifescan; Burnaby, BC). Mice were anesthetized with inhalable isoflurane and received transplants of ~1.9 million stage 6 hES cell–derived cells beneath the left kidney capsule. In some cases, transplants were performed in diabetic mice (blood glucose >18 mmol/l) after treatment with streptozotocin (STZ; 175 mg/kg). After transplantation, all mice were treated with oral enrofloxacin (Bayer Animal Health. Shawnee Mission, KS) for 1 week (50 mg/500 ml in drinking water). In diabetic animals a 30-day, slow-release insulin pellet (LinBit; Linshin Canada; Toronto, ON) was implanted subcutaneously to maintain normoglycemia.

In vivo analysis of transplanted cells. Metabolic analyses were performed in conscious, restrained mice on the indicated days. Details of metabolic studies can be found in the supplemental data.

RESULTS

Development of an α-cell differentiation protocol. Significant advances in the formation of pancreatic endocrine cells from hES cells have been recently achieved by attempting to mimic the natural stepwise development of the endocrine pancreas in vitro (4–6). Using a similar stepwise approach, we performed a combination of small molecule screening and empirical testing of known endocrine morphogens to develop a differentiation protocol leading to the formation of mature α-cells (Fig. 1*A*). To improve on previous attempts of in vitro endocrine cell formation, adherent cultures were differentiated under feeder-free conditions in the absence of FBS. Our protocol was divided into six distinct stages, mimicking the stepwise development of endogenous human islets. To specify the anterior primitive streak region, referred to here as mesoendoderm, stage 1 cells were cultured in the presence of Wnt-3A, FGF2, and activin A (10–12). Robust expression of *CD184* (*CXCR4*), *FOXA2*, and *SOX17* suggested mesoendoderm formation (13–15), (Fig. 1*B* and supplementary Fig. S1*A* and *B*), whereas low expression levels of *AFP*, *SOX7*, and *BRY*(T) suggested a lack of visceral endoderm (16) and mesoderm formation (supplementary Fig. S1*A*). Promoting fibroblast growth factor

(FGF) and retinoic acid signaling while restricting sonic hedgehog (SHH) and BMP signaling can specify the pancreatic domain from the gut tube (17–20) and may reduce formation of hepatocytes (21). Furthermore, inhibition of BMP signaling can promote the formation of endocrine cells in the developing zebrafish (22). Thus, during stages 2 and 3, cells were exposed to FGF7, cyclopamine, retinoic acid, and Noggin, resulting in the upregulation of foregut endoderm and pancreatic precursor markers, including *HNF4α* and *PDX-1* (supplementary Fig. S1*C*). Removal of Noggin at later stages of the protocol may allow for sufficient BMP signaling to facilitate the formation and maturation of α-cells (23).

Disruption of Notch and TGF-β signaling has been shown to promote the pancreatic endocrine cell lineage, partially through upregulation of *NGN3* expression (24) and by redirecting pancreatic epithelial cells that would otherwise differentiate into ductal cells toward an endocrine fate (25). We performed a targeted screening of 160 cell-permeable kinase inhibitors at stages 3 and 4 of differentiation and identified 2-(3-[6-Methylpyridin-2-yl]-1*H*-pyrazol-4-yl)-1,5-naphthyridine (ALK5 inhibitor II) as a potent inducer of insulin and glucagon message (supplementary Fig. S2*A* and *C*), likely via upregulation of the transcription factors *NeuroD* and *NGN3* (supplementary Figs. S1*D* and S2*B*, *D*, and *E*). Similar results were obtained using [3-(Pyridin-2-yl)-4-(4-quinonyl)]-1*H*-pyrazole (ALK5 inhibitor I), although the upregulation of these markers was not as dramatic (data not shown). Addition of the notch inhibitor DAPT at stage 4 resulted in a small increase in expression of *NeuroD* and *NGN3* expression, but no significant effect on the expression of insulin and glucagon (data not shown). Thus, in stage 4, inhibition of TGF-β signaling using ALK5 inhibitor II, as well as Notch signaling using DAPT, progressed cells to a pancreatic endocrine phenotype. The endocrine cell markers *PAX4*, *PAX6*, and *NKX2.2* were highly upregulated at stage 4 (supplementary Fig. S1*C*) as were the number of *NGN3*-positive cells within the culture (supplementary Fig. S2*E*). Furthermore, ALK5 inhibitor II resulted in a concentration-dependent increase in expression of the α-cell–enriched transcription factor *ARX* (supplementary Fig. S2*D*) thus potentially contributing to the eventual maturation of the cells toward an α-cell phenotype. As further evidence of the transition of the differentiating cells away from a β-cell phenotype, *NKX6.1* message was undetectable in the differentiating cell population (supplementary Fig. S1*C*) and we were unable to detect NKX6.1 immunofluorescence in PDX-1-positive cells within the culture at this stage (supplementary Fig. S1*E*). Previous reports have shown that NKX6.1 null mice lack pancreatic β-cells (26), and as early as 10 weeks of gestation and in the adult human islet, expression of NKX6.1 becomes limited to β-cells and is absent from glucagon-expressing α-cells (27).

The expression of both glucagon (*GCG*) and insulin (*INS*) was upregulated at stage 5, with continued inhibition of TGF-β receptor signaling (Figs. 1*C* and supplementary Fig. S2*C*). During stage 6, we observed the spontaneous formation of clusters that resembled human islets in both size and shape (Fig. 1*D*). These clusters contained significantly higher levels of *INS* and *GCG* mRNA compared with stage 6 cells that remained part of the monolayer (Fig. 1*C*) and were highly enriched for the panendocrine cell marker synaptophysin (Fig. 2*A*). In contrast to adult human islets (Fig. 2*B*), significant coex-

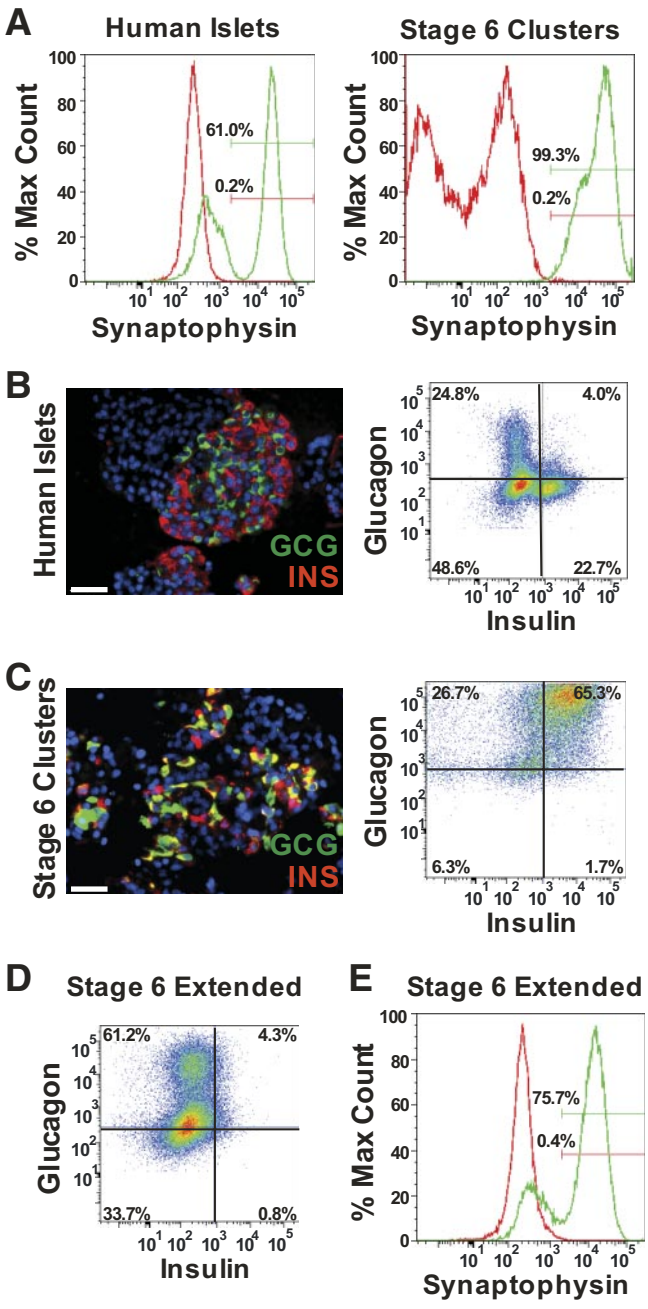

FIG. 2. Morphologic characterization of hES cell–derived cells. *A*: Representative flow analysis of synaptophysin expression in isolated human islets (*left*) and stage 6 clusters (*right*). Isotype shown in *red*. *B*: Representative glucagon (GCG) and insulin (INS) immunofluorescence images in paraffin-sectioned adult human islets (*left*) and flow data from dispersed adult human islets (*right*). GCG immunoreactivity is shown in *green* and INS immunoreactivity is shown in *red*. Scale bar, 50 μm. Quadrant gates set using isotype controls (not shown). *C*: Representative GCG and INS immunofluorescence images in paraffin-sectioned stage 6 clusters (*left*) and flow data from dispersed stage 6 clusters (*right*). GCG immunoreactivity is shown in *green* and INS immunoreactivity is shown in *red*. Cells expressing both GCG and INS are shown in *yellow*. Scale bar, 50 μm. Images in *B* and *C* include a DAPI nuclear stain (blue). Quadrant gates set using isotype controls (not shown). *D*: Representative GCG and INS flow data from dispersed stage 6 clusters after an extended 4-week culture period. Quadrant gates set using isotype controls (not shown). *E*: Representative synaptophysin expression in stage 6 clusters dispersed after an extended 4-week culture period. Isotype shown in *red*. (A high-quality color representation of this figure is available in the online issue.)

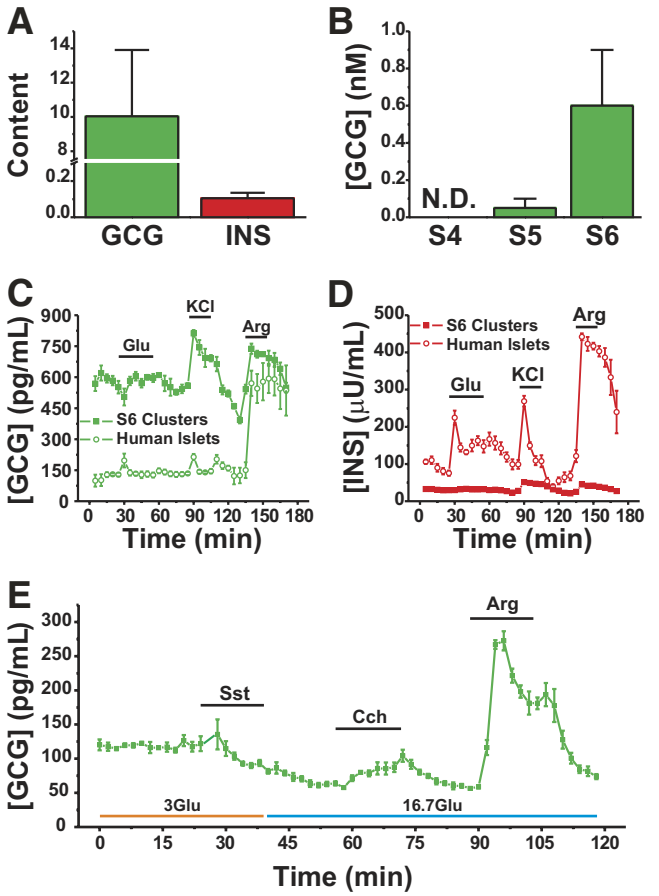

FIG. 3. Hormone content and secretion kinetics of hES cell–derived cells. *A*: Glucagon and insulin content of stage 6 clusters, normalized for total DNA content and expressed as fold difference over human islets (n = 3 samples for ES-derived cells and n = 8 for human islets). Error bars indicate SE. *B*: Twenty-four hour bioactive glucagon release from hES cells at indicated differentiation stages (n = 2). N.D., not detected. *C* and *D*: Glucagon (*C*) and insulin (*D*) secretion from perifused human islets and stage 6 clusters (n = 4 chambers for each) in response to 15 mmol/l glucose (Glu), 30 mmol/l KCl and 15 mmol/l arginine (Arg). *E*: Glucagon secretion from perifused stage 6 clusters (n = 4 chambers) in response to 3 mmol/l glucose (3Glu) or 16.7 mmol/l (16.7Glu) with or without 1 μmol/l of the somatostatin analog octreotide (Sst), 100 μmol/l carbachol (Cch), or 15 mmol/l arginine (Arg) as indicated. (A high-quality color representation of this figure is available in the online issue.)

pression of insulin and glucagon was detected by both flow cytometry and immunofluorescence (Fig. 2*C*). Colocalization of C-peptide and insulin immunoreactivities (supplementary Fig. S3*A* and *B*) indicates that the observed insulin immunoreactivity is unlikely to be caused by uptake of insulin from the culture medium. In stage 6, cells within the clusters expressed additional islet hormones, including somatostatin and ghrelin (supplementary Fig. S3*C* and *D*). Glucagon-positive cells exhibited a subcellular morphology similar to that of human α-cells (supplementary Fig. S3*E* and *F*).

In vitro characterization of differentiated cells. Glucagon and insulin protein content were ~10-fold higher and 10-fold lower in the stage 6 clusters than in human islets, respectively (Fig. 3*A*). Biologically active glucagon secretion was first detected at stage 5 and increased in stage 6 (Fig. 3*B*). Stage 6 clusters exhibited insulin secretion in response to KCl, and arginine, albeit at quite low levels (Fig. 3*D*), with no significant response to glucose (Fig. 3*D*). In some cases, basal secretion of glucagon in low glucose was significantly greater than that observed in human islets (Fig. 3*C*), although in some cases, basal glucagon secretion was similar (Fig. 3*E*). Both KCl and arginine stimulated glucagon secretion (Fig. 3*C* and *E*) as did the acetylcholine analog carbachol (Fig. 3*E*). Glucagon release was diminished in the presence of the somatostatin analog octreotide or high glucose, suggesting that glucagon secretion can be physiologically regulated in these cells (Fig. 3*E*). After extended culture of stage 6 clusters in vitro, the percentage of insulin-positive and insulin/glucagon copositive cells decreased markedly. Conversely, the percentage of glucagon-positive cells was increased (Fig. 2*D*), whereas the proportion of cells expressing the endocrine marker synaptophysin remained high at ~75% (Fig. 2*E*).

In vivo characterization of differentiated cells. To test whether stage 6 clusters were lineage-restricted to become α-cells and to assess the physiologic regulation of glucagon secretion from these cells, normoglycemic B6.129S7-Rag^{Tm1Mom}/J mice were transplanted with ~1.9 × 10^6 stage 6 clusters. Animals were followed with routine blood glucose tracking and additional metabolic tests for up to 5 months after transplantation. Cell recipients showed occasionally elevated 4-h fasted blood glucose levels compared with control animals (Fig. 4*A*). At 99 days after transplant, prolonged (~16 h) fasting resulted in elevated plasma glucagon levels in cell recipients (399.2 ± 32.5 pg/ml) compared with control animals, where glucagon levels were largely undetectable (<40 pg/ml). Feeding significantly reduced plasma glucagon to 227.7 ± 46.3 pg/ml in cell transplant recipients (Fig. 4*B*). Importantly, postprandial blood glucose levels were not significantly different between groups (Fig. 4*B*).

We tested the ability of the engrafted hES cell–derived glucagon-expressing cells to respond to known α-cell secretion stimuli. In response to an intraperitoneal arginine bolus performed at 62 days after transplant, plasma glucagon levels in cell recipients rose significantly from 88.1 ± 15.3 pg/ml to 1,060.4 ± 83.6 pg/ml. In contrast, control animals mounted a minimal glucagon response to this challenge (Fig. 4*D*; <40 pg/ml at basal to 46.7 ± 4.4 pg/ml at 7 min). Despite the robust glucagon secretion observed in cell recipients, blood glucose levels increased only minimally by 13.8 ± 6.9% within the first 7 min after arginine administration. Control animals exhibited a 47.6 ± 15.9% increase in blood glucose levels in this same timeframe (Fig. 4*C*). In addition, cell recipients exhibited a more marked reduction in blood glucose levels at later time points than control animals, reaching a minimum of 58.7 ± 7.7% of basal vs. 71.4 ± 9.0% of basal for controls at 30 min postinjection. Pancreatic insulin secretion was not significantly different between groups (Fig. 4*C*, inset).

Interestingly, plasma glucagon-like peptide-1 (GLP-1) levels were significantly elevated in cell recipients after arginine administration (54.2 ± 8.2 pg/ml vs. 7.5 ± 0.89 pg/ml in control animals at 7 min (supplementary Fig. S4*A*). GLP-1 secretion was stimulated by feeding in both groups. However, although basal plasma GLP-1 levels were higher in cell recipients, stimulated levels remained in the physiologic range and were not significantly different from control animals (supplementary Fig. S4*B*).

In response to an oral glucose challenge performed at 77 days after transplant, no differences were observed in peak blood glucose, glucose clearance, or insulin secretion between groups (Fig. 4*E*). To test whether chronic hyperglucagonemia in cell transplant recipients induced

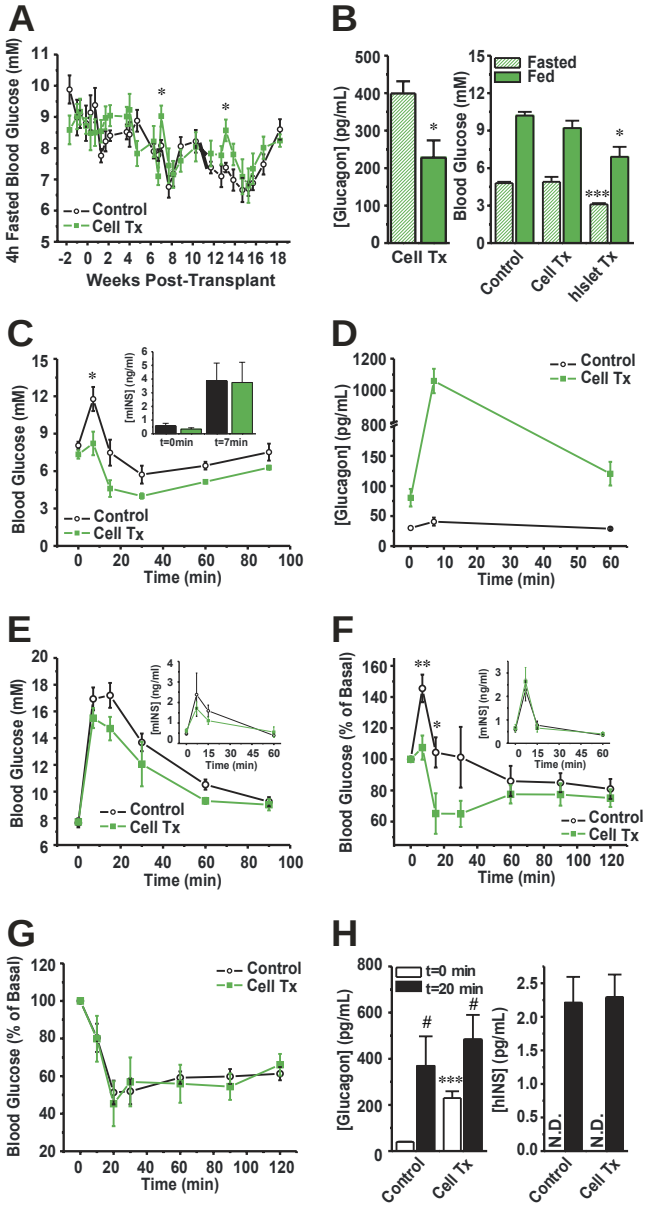

FIG. 4. Transplantation of hES cell–derived cells induces hyperglucagonemia and glucagon intolerance. *A*: Blood glucose levels after a 4-h morning fast. *B*: Blood glucose and plasma glucagon levels after an overnight fast and after 45-min refeeding period at 99 days after transplant (Tx). Glucagon was below the level of detection for control and human islet Tx groups (<40 pg/ml). *C*: Blood glucose and plasma mouse insulin levels (mINS; inset) at day 62 after transplant in response to intraperitoneal arginine injection (2 g/kg). *D*: Plasma glucagon levels for intraperitoneally arginine test shown in panel *C*. *E*: Blood glucose and plasma mouse insulin levels (mINS; inset) after a 4-h morning fast at day 77 after transplant in response to oral glucose challenge (2 g/kg). *F*: Blood glucose and plasma mouse insulin levels (mINS; inset) at day 92 after transplant in response to intraperitoneal glucagon injection (1 μg/kg). *G*: Whole body insulin sensitivity was assessed by injecting recombinant human insulin (0.4 units/kg) at day 114 after transplant. *H*: Plasma immunoreactive glucagon (*left*) and insulin (*right*) levels in response to insulin injection shown in panel *G*. n = 5–7 animals/group; *P < 0.05, **P < 0.01, ***P < 0.001 vs. control; #P < 0.05 vs. respective 0-min time point (Student t test). N.D., not detected. (A high-quality color representation of this figure is available in the online issue.)

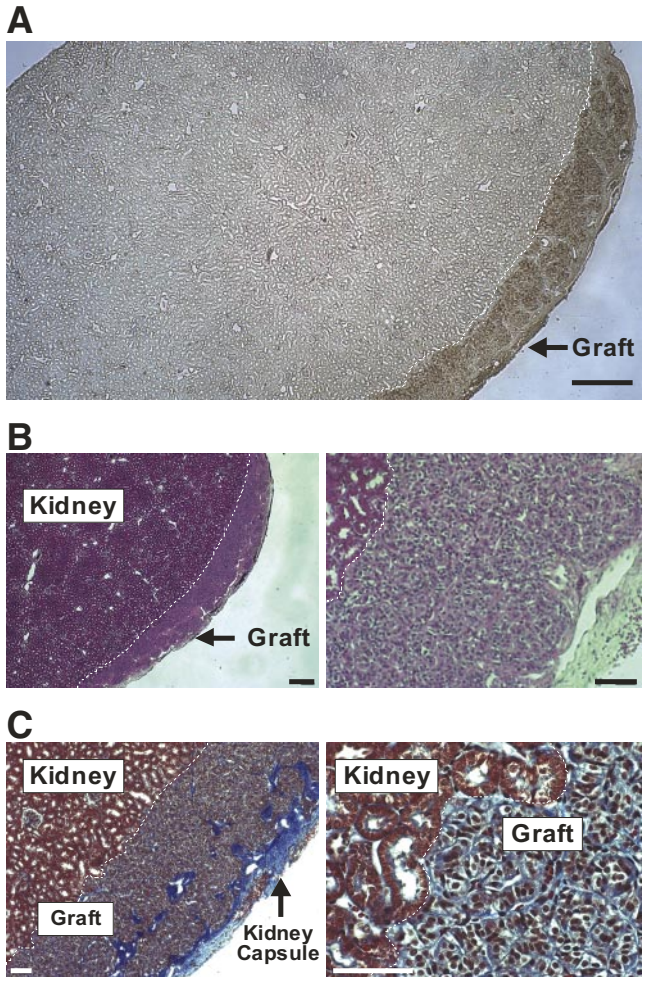

FIG. 5. Gross histology of transplanted hES cell–derived cells. Grafts were harvested from hES cell recipients at day 125 after transplant. *A*: Representative image of engrafted kidney section after DAB staining for glucagon. Scale bar = 1 mm. *B*: Representative images of hematoxylin-eosin staining at (*left*) low and (*right*) high magnification. Scale bars = 1 mm for low magnification image and 50 μm for high magnification image. *C*: Representative images of Masson's trichrome staining at (*left*) low and (*right*) high magnification. Collagen fibers are stained in *blue*. Scale bars = 100 μm. In all panels, *white dotted line* delineates kidney-graft border. (A high-quality color representation of this figure is available in the online issue.)

compensatory glucagon resistance, we performed an intraperitoneal glucagon tolerance test at 92 days after transplant. Control mice exhibited a significant increase (45.5 ± 8.9%) in blood glucose at 7 min, although cell recipients did not (Fig. 4*F*). However, both groups of mice mounted an equal pancreatic insulin response (Fig. 4*F*, inset). Furthermore, although blood glucose had returned to basal in control mice by 30 min (101.3 ± 19.5% of basal), cell recipients exhibited an exaggerated decline in blood glucose levels at 30 min (65.0 ± 8.4% of basal; Fig. 4*F*). At 114 days after transplant, control and cell recipient mice displayed similar insulin sensitivity (Fig. 4*G*), and both groups exhibited a robust hypoglycemia-induced increase in plasma glucagon levels (368.9 ± 128.2 pg/ml for controls, n = 5; 483.2 ± 106.8 pg/ml for cell recipients; n = 7; Fig. 4*H*, *left*) in response to a similar level of hyperinsulinemia (Fig. 4*H*, *right*). Thus, the primary metabolic phenotype observed in cell recipients was chronic hyperglucagonemia together with mild glucagon resistance.

Characterization of engrafted hES-derived cells. At ~4 months after transplant, engrafted cells were harvested and characterized in comparison with pretransplant stage 6 clusters. Gross histologic analysis of the graft revealed that most of the cells express glucagon (Fig. 5*A*).

Hematoxylin-eosin staining revealed characteristic endocrine cell morphology within the graft, whereas Masson's trichrome staining indicated that areas not occupied by glucagon-positive cells were largely occupied by connective tissue (Fig. 5*B*–*C*). As in stage 6 clusters that underwent extended in vitro culture, transplanted cells lost insulin expression while maintaining robust glucagon expression (Fig. 6*A*). This loss of polyhormonal islet endocrine cells is also observed in the developing human pancreas (28).

The transcription factor ARX is critical for the development and maintenance of the α-cell phenotype (29,30). ARX immunoreactivity was extensive within the stage 6 clusters and the transplanted cells (Fig. 6*B*). Despite evidence of insulin immunoreactivity within the stage 6 clusters, nuclear-localized PDX-1 immunoreactivity was not observed in stage 6 clusters and was completely absent within the graft (Fig. 6*C*). Furthermore, glucagon expression in the grafts was colocalized with the prohormone processing enzyme PC2 (Fig. 6*D*), which mediates glucagon release from the proglucagon precursor in endogenous α-cells, but not with the alternate processing enzyme PC1/3. The lineage fate of stage 6 clusters was not dependent on the glycemic state of the animal, as clusters transplanted into streptozotocin-induced diabetic animals also developed an α-cell phenotype. As such, these cells were unable to reverse hyperglycemia (supplementary Fig. S5*A*) but were capable of arginine-stimulated glucagon secretion (supplementary Fig. S5*B* and *C*). Moreover, these engrafted cells likewise lost insulin while maintaining glucagon expression (supplementary Fig. S5*D*). To further characterize the hES cell–derived cells within the graft, mRNA expression levels of 84 genes were assessed in grafts collected ~5 months after transplant and compared with adult human islets (supplementary Table S1). In agreement with immunostaining observations, *GCG* and *ARX* mRNA levels in the engrafted cells were upregulated 37.14 ± 3.51 and 82.53 ± 10.09-fold, respectively, whereas *INS* message was nearly undetectable. Interestingly, *MAFA* mRNA was downregulated 40.53 ± 2.32-fold and *NKX6.1* message was undetectable, providing further evidence of α-cell formation.

Tumorigenicity remains a major concern facing hES cell–based therapies, and previous studies have shown that transplantation of endocrine precursor cells can result in teratoma formation in a significant percentage of examined grafts (8). To test the proliferative potential of our transplanted hES cells, we examined PCNA immunoreactivity within the stage 6 clusters and the engrafted kidney. Although no features of teratomas or other tumors were observed in any of the 12 examined engrafted kidneys (Fig. 5*A*–*C*), proliferating cells were observed within the clusters both before and after transplantation (Fig. 6*E*).

To assess whether bioactive glucagon release from the transplanted cells had reduced the demand for pancreatic glucagon, pancreatic α-cell mass was quantified. We noted a significant decrease in α-cell mass in cell recipients (241 ± 35 μg/pancreas; $n = 6$) versus control animals (393 ± 57 μg/pancreas; $n = 5$; supplementary Fig. S6).

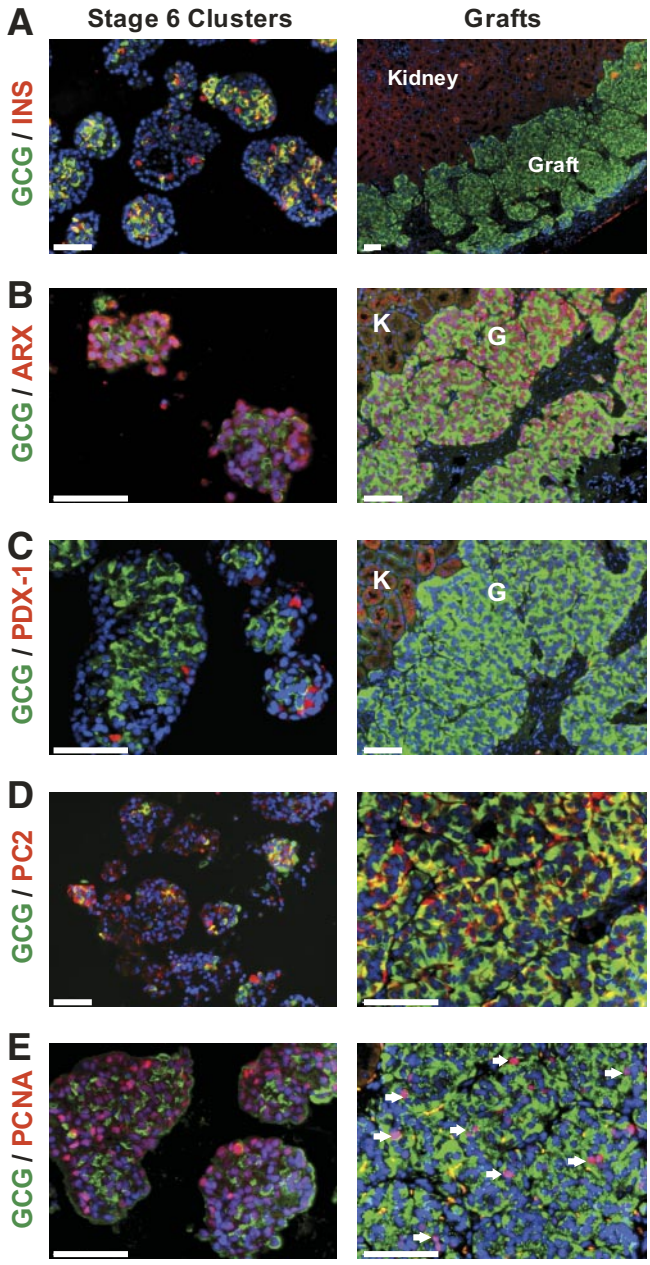

FIG. 6. The α-cell phenotype is enriched after in vivo transplantation. Double immunofluorescence was performed on pretransplant stage 6 clusters and grafts collected 125 days after transplantation. Representative images are shown. *A*: Insulin (INS; *red*) expression is largely lost after transplantation whereas glucagon (GCG; *green*) expression predominates. *B*: GCG (*green*) and ARX (*red*) coexpression is maintained in stage 6 hES cell–derived cells before and after transplantation. *C*: PDX-1 (*red*) expression is distinct from glucagon (*green*) expression in stage 6 clusters, and is absent in grafts. *D*: Coexpression of glucagon (*green*) and PC2 (*red*) is increased in retrieved grafts compared with stage 6 clusters. *E*: Robust PCNA immunoreactivity (*red*) is observed in many glucagon-positive cells (*green*) in stage 6 clusters and after transplantation (see *arrows*). Scale bars, 100 μm. Images include a DAPI nuclear stain (*blue*). Kidney and graft tissues are denoted by K and G, respectively, in panels *B* and *C*. (A high-quality color representation of this figure is available in the online issue.)

DISCUSSION

The developmental program driving the formation of mature endocrine islets, especially in humans, is not fully understood. A number of critical signaling pathways and transcription factors have been identified and their roles elucidated through genetic knockout and pharmacologic activation/inhibition experiments; however, the temporal and spatial cues that result in proper development are complex. For example, although inhibition of BMP signaling in the early mouse embryo increases *Pdx-1* and *Hnf6* expression at the expense of liver-specific genes, inhibi-

tion of BMP signaling only hours later can reduce both *Pdx-1* and *Hnf6* expression (21). Despite this temporal complexity, significant progress has recently been made in the differentiation of hES cells to definitive endoderm (2,3). This has facilitated the development of protocols that promote further differentiation to endocrine precursor cell types (4,8). Here we report the formation of mature glucagon-secreting α-cells from hES cells. Characterizing expression levels of several endocrine cell markers at each stage of differentiation aided in the discovery of culture conditions that resulted in the efficient formation of pancreatic endocrine cells. Indeed, this protocol resulted in 75% of differentiated cells expressing the endocrine marker synaptophysin. Lineage specification toward α-cells was determined by positive immunoreactivity using an antibody specific for fully processed glucagon and by using a cell-based bioassay that recognizes activation of the human glucagon receptor. The observation that stage 6 clusters matured to α-cells in vitro and in vivo, regardless of the glycemic state of the cell recipient, suggests that lineage specification likely occurs at or before this stage of the differentiation protocol. Therefore, the creation of β-cells from a similar differentiation protocol may require culture manipulations preceding this last differentiation stage.

Pancreatic α- and β-cells likely arise from the same *NGN3*-expressing progenitor cell population (31), and the coexpression of insulin and glucagon within the developing human and rodent pancreas has been reported by several groups (28,32). Although one study has suggested that these dual hormone expressing cells are unlikely to contribute to the adult α-cell or β-cell pool, this conclusion was based on potentially incomplete labeling during lineage tracing of developing α- and β-cells (33). The existence of a subpopulation of dual expressing cells contributing to the mature α-cell population in mice cannot be ruled out based on this study alone, nor does any evidence exist for the inability of these dual expressing cells to contribute to the development of mature endocrine cells in the human islet. Although the fate of these dual-expressing cells remains controversial, it is clear that these cells arise from the same progenitor pool as the adult unihormonal cells as *NGN3* expression is likely absolutely required for the formation of pancreatic endocrine cells (34,35). Temporal regulation of *NGN3* expression can greatly influence the α- to β-cell ratio, with early expression preferentially forming α cells (36). Given the short duration of our differentiation protocol (26 days through the end of stage 6), subtle changes in the temporal activation of transcription factors could dramatically alter the ratio of α- to β-cells created. Furthermore, inhibition of TGF-β signaling, which resulted in an upregulation of *NGN3* and *ARX* expression in our model, has been implicated in shifting the balanced formation of α- and β-cells toward a predominately glucagon-positive population (37). Our data suggest that there exists a narrow competence window at stage 4 for the inhibition of TGF-β signaling to induce the expression of *NGN3* as well as the endocrine hormones insulin and glucagon, with Alk5 inhibitor II increasing expression of these genes when added at stage 4 (supplementary Fig. S2*A* and *C*), but not at stage 3 (data not shown) or stage 5 alone.

Downstream of NGN3, the transcription factors PAX4 and ARX are likewise known to play critical roles in the proper development of the islet. PAX4 deficiency results in an absence of β-cells, but a striking increase in the number of α-cells (38). Conversely, ARX-deficient mice show a dramatic increase in β- and δ-cell formation at the expense of α-cells (29), suggesting that PAX4 and ARX perform opposing roles in the maturation of endocrine precursors. Indeed, these two transcription factors have been shown to inhibit the expression of each other by directly binding to the promoter region of the opposing transcription factor (30). Although we observed levels of *PAX4* gene expression during hES cell differentiation that exceed that found in adult human islets (~1.5 fold; supplementary Table S1), expression of *ARX* was much more highly upregulated (~82-fold; Table S1), suggesting that the balance of these two transcription factors is overwhelmingly tipped toward an α-cell phenotype. In this regard, constitutive overexpression of *PAX4* in differentiating hES cells can improve the efficiency of β-cell formation (39), and conditional expression of *PAX4* in endogenous α-cells that contain normal ARX expression levels results in their transdifferentiation to β-cells (40). Thus, the high level of *ARX* expression coupled with low expression of *INS*, *PDX-1*, and the β-cell–specific transcription factors *MafA*, *PAX4*, and *NKX6.1* (26,41) (Fig. S1*C*), further highlight the formation of α-cells with this protocol.

In the pancreatic α-cell, coexpression of proglucagon with PC2 results primarily in the formation of mature glucagon. Conversely, in PC1/3-expressing cells, such as the gastrointestinal L cells, proglucagon is processed to yield GLP-1, GLP-2, glicentin, and oxyntomodulin. In some cells in the stage 6 clusters, glucagon immunoreactivity colocalized with either PC1/3 or PC2, suggesting that any or all proglucagon-derived peptides may be produced. Indeed, cell recipients had significantly elevated plasma GLP-1 levels, suggesting that GLP-1 may be secreted from the engrafted cells. Previous studies have shown that some early mouse embryonic glucagon-expressing cells also express PC1/3 and thus likely produce GLP-1, and some have suggested that production within the developing islet may be important for mature islet formation (42). GLP-1 production from the graft may be from a population of α-cells that have yet to mature or form a separate differentiated cell lineage. The separate development of glucagon and GLP-1–expressing cells within the graft is supported by the appropriately opposite regulation of glucagon and GLP-1 secretion in cell transplant recipients after feeding. Furthermore, peak plasma GLP-1 levels after arginine administration were similar at day 9 and day 62, whereas peak plasma glucagon levels in response to arginine administration increased fourfold over this timeframe, suggesting that the GLP-1–producing cells may have developed by stage 6, whereas glucagon-producing cells required more time to mature.

In our study, we show that glucagon secretion from hES-derived cells was increased by fasting and hypoglycemia and diminished by elevated glucose concentrations. Moreover, as with native α-cells, arginine was a potent stimulant of glucagon secretion both in vitro and in vivo. Both fasting and fed plasma glucagon levels were significantly higher in cell recipients compared with control animals. Although hypoglycemia induces glucagon secretion in vivo, glucose itself can stimulate glucagon secretion in isolated α-cells (43). In both humans and rodents, insulin plays a key role in regulating glucagon secretion in vivo (44,45), possibly via creation of a critical microenvironment in which insulin secreted from the β-cells acts on adjacent α-cells to inhibit glucagon secretion. The increased basal glucagon secretion observed in our study

may result from reduced or absent negative feedback due to a lack of local insulin production. This excessive basal glucagon secretion likely contributed to the observed development of mild glucagon resistance in cell recipients. Despite glucagon resistance, cell recipients maintained normal glucoregulatory responses to fasting, feeding, and nutrient administration. Taken together with our bioassay data confirming that conditioned media from stage 6 clusters activated the glucagon receptor, and our observations of decreased pancreatic α-cell mass in cell recipients, these data confirm that the glucagon secreted from hES-derived cells was mature, bioactive, and secreted in response to physiologic stimuli.

We previously showed that transplantation of α-cell–like αTC-1 cells into normoglycemic mice results in chronic elevation of fasting blood glucose and impaired glucose tolerance (46). In contrast, recipients of the differentiated hES cells displayed only occasionally elevated fasting blood glucose and had normal glucose tolerance, suggesting that hES-derived cells possess more physiologically-regulated secretion of glucagon than do αTC-1 cells. Given that a lack of suppression of glucagon secretion contributes to hyperglycemia in individuals with type 2 diabetes (47), the development of a physiologically regulated human α-cell line may have significant utility as a screening tool for the identification of novel therapeutics that suppress glucagon secretion.

As the burgeoning field of regenerative medicine continues to mature, a method for the formation of terminally differentiated, appropriately regulated, nontumorigenic pancreatic endocrine cells is highly desirable. We demonstrate here that with appropriate and defined manipulation of culture conditions, hES cells can be differentiated into functional α-cells. Through a rigorous in vitro and in vivo characterization, we show that these hES-derived endocrine cells secrete biologically active glucagon in response to known glucagon secretagogues and, importantly, they are not tumorigenic. There is increasing evidence to suggest that α-cells exhibit a unique plasticity that allows for their conversion to insulin-producing β-cells under certain conditions. The ectopic expression of *pax4* (40) or ablation of *men1* expression (48) in α-cells facilitates their transdifferentiation to β-cells. Furthermore, Herrera and colleagues recently demonstrated that near total β-cell ablation results in the conversion of pre-existing α-cells to β-cells (49). In light of these recent findings, our hES cell–derived α-cells may serve as a novel starting material for the identification of small molecules that promote the conversion of this cell type to β-cells, either in our in vitro culture system or in vivo. Given that transdifferentiation of exocrine cells to β-cells has been recently demonstrated in vivo (50), we speculate that it may be possible to identify compounds that convert α-cells to β-cells as a novel strategy for the treatment of diabetes.

ACKNOWLEDGMENTS

Financial support for this project was provided by the Stem Cell Network. M.J.R. is supported by the Michael Smith Foundation for Health Research (MSFHR), the Canadian Diabetes Association, the Stem Cell Network, and the Juvenile Diabetes Research Foundation. T.J.K. is a MSFHR senior scholar.

A.R. and F.K. are employees of Centocor Research and Development. T.J.K. has received financial support for this project from Centocor R&D. No other potential conflicts of interest relevant to this article were reported.

A.R. and R.D.W. researched data and reviewed/edited the manuscript. M.J.R. researched data and wrote the manuscript. F.K. researched data. Z.A. contributed human islets. G.L.W. contributed human islets and reviewed/edited the manuscript. T.J.K. reviewed/edited the manuscript.

The authors would like to acknowledge the expert technical assistance contributed by Ali Asadi, Travis Webber, Anastasia Vlasova, Christine Donald, and Madeleine Speck, all from the University of British Columbia, along with Ramie Fung from Centocor Research and Development. The authors also thank Dr. Jim Johnson and Betty Hu from the University of British Columbia for assistance with perifusion experiments. They also thank Christopher Cahill at The Joslin Diabetes Center for assistance preparing TEM images.

REFERENCES

1. Alper J. Geron gets green light for human trial of ES cell-derived product. Nat Biotechnol 2009;27:213–214
2. Borowiak M, Maehr R, Chen S, Chen AE, Tang W, Fox JL, Schreiber SL, Melton DA. Small molecules efficiently direct endodermal differentiation of mouse and human embryonic stem cells. Cell Stem Cell 2009;4:348–358
3. D'Amour, KA, Agulnick AD, Eliazer S, Kelly OG, Kroon E, Baetge EE. Efficient differentiation of human embryonic stem cells to definitive endoderm. Nat Biotechnol 2005;23:1534–1541
4. D'Amour KA, Bang AG, Eliazer S, Kelly OG, Agulnick AD, Smart NG, Moorman MA, Kroon E, Carpenter MK, Baetge EE. Production of pancreatic hormone-expressing endocrine cells from human embryonic stem cells. Nat Biotechnol 2006;24:1392–1401
5. Jiang J, Au M, Lu K, Eshpeter A, Korbutt G, Fisk G, Majumdar AS. Generation of insulin-producing islet-like clusters from human embryonic stem cells. Stem Cells 2007;25:1940–1953
6. Jiang W, Shi Y, Zhao D, Chen S, Yong J, Zhang J, Qing T, Sun X, Zhang P, Ding M, Li D, Deng H. In vitro derivation of functional insulin-producing cells from human embryonic stem cells. Cell Res 2007;17:333–344
7. Shim JH, Kim SE, Woo DH, Kim SK, Oh CH, McKay R, Kim JH. Directed differentiation of human embryonic stem cells towards a pancreatic cell fate. Diabetologia 2007;50:1228–1238
8. Kroon E, Martinson LA, Kadoya K, Bang AG, Kelly OG, Eliazer S, Young H, Richardson M, Smart NG, Cunningham J, Agulnick AD, D'Amour KA, Carpenter MK, Baetge EE. Pancreatic endoderm derived from human embryonic stem cells generates glucose-responsive insulin-secreting cells in vivo. Nat Biotechnol 2008;26:443–452
9. Xu C, Inokuma MS, Denham J, Golds K, Kundu P, Gold JD, Carpenter MK. Feeder-free growth of undifferentiated human embryonic stem cells. Nat Biotechnol 2001;19:971–974
10. Kubo A, Shinozaki K, Shannon JM, Kouskoff V, Kennedy M, Woo S, Fehling HJ, Keller G. Development of definitive endoderm from embryonic stem cells in culture. Development 2004;131:1651–1662
11. Gadue P, Huber TL, Paddison PJ, Keller GM. Wnt and TGF-β signaling are required for the induction of an in vitro model of primitive streak formation using embryonic stem cells. Proc Natl Acad Sci U S A 2006;103:16806–16811
12. Morrison GM, Oikonomopoulou I, Migueles RP, Soneji S, Livigni A, Enver T, Brickman JM. Anterior definitive endoderm from ESCs reveals a role for FGF signaling. Cell Stem Cell 2008;3:402–415
13. McGrath KE, Koniski AD, Maltby KM, McGann JK, Palis J. Embryonic expression and function of the chemokine SDF-1 and its receptor, CXCR4. Dev Biol 1999;213:442–456
14. Monaghan AP, Kaestner KH, Grau E, Schutz G. Postimplantation expression patterns indicate a role for the mouse forkhead/HNF-3 α, β and γ genes in determination of the definitive endoderm, chordamesoderm and neuroectoderm. Development 1993;119:567–578
15. Kanai-Azuma M, Kanai Y, Gad JM, Tajima Y, Taya C, Kurohmaru M, Sanai Y, Yonekawa H, Yazaki K, Tam PP, Hayashi Y. Depletion of definitive gut endoderm in Sox17-null mutant mice. Development 2002;129:2367–2379
16. Dziadek MA, Andrews GK. Tissue specificity of α-fetoprotein messenger RNA expression during mouse embryogenesis. EMBO J 1983;2:549–554
17. Norgaard GA, Jensen JN, Jensen J. FGF10 signaling maintains the pancre-

atic progenitor cell state revealing a novel role of Notch in organ development. Dev Biol 2003;264:323–338
18. Stafford D, Prince VE. Retinoic acid signaling is required for a critical early step in zebrafish pancreatic development. Curr Biol 2002;12:1215–1220
19. Hebrok M, Kim SK, St JB, McMahon AP, Melton DA. Regulation of pancreas development by hedgehog signaling. Development 2000;127: 4905–4913
20. Rossi JM, Dunn NR, Hogan BL, Zaret KS. Distinct mesodermal signals, including BMPs from the septum transversum mesenchyme, are required in combination for hepatogenesis from the endoderm. Genes Dev 2001;15: 1998–2009
21. Wandzioch E, Zaret KS. Dynamic signaling network for the specification of embryonic pancreas and liver progenitors. Science 2009;324:1707–1710
22. Chung WS, Andersson O, Row R, Kimelman D, Stainier DY. Suppression of Alk8-mediated Bmp signaling cell-autonomously induces pancreatic β-cells in zebrafish. Proc Natl Acad Sci U S A 2010;107:1142–1147
23. Hua H, Sarvetnick N. Expression of Id1 in adult, regenerating and developing pancreas. Endocrine 2007;32:280–286
24. Jensen J, Pedersen EE, Galante P, Hald J, Heller RS, Ishibashi M, Kageyama R, Guillemot F, Serup P, Madsen OD. Control of endodermal endocrine development by Hes-1. Nat Genet 2000;24:36–44
25. Tulachan SS, Tei E, Hembree M, Crisera C, Prasadan K, Koizumi M, Shah S, Guo P, Bottinger E, Gittes GK. TGF-β isoform signaling regulates secondary transition and mesenchymal-induced endocrine development in the embryonic mouse pancreas. Dev Biol 2007;305:508–521
26. Sander M, Sussel L, Conners J, Scheel D, Kalamaras J, Dela CF, Schwitzgebel V, Hayes-Jordan A, German M. Homeobox gene Nkx6.1 lies downstream of Nkx2.2 in the major pathway of β-cell formation in the pancreas. Development 2000;127:5533–5540
27. Lyttle BM, Li J, Krishnamurthy M, Fellows F, Wheeler MB, Goodyer CG, Wang R. Transcription factor expression in the developing human fetal endocrine pancreas. Diabetologia 2008;51:1169–1180
28. De Krijger RR, Aanstoot HJ, Kranenburg G, Reinhard M, Visser WJ, Bruining GJ. The midgestational human fetal pancreas contains cells coexpressing islet hormones. Dev Biol 1992;153:368–375
29. Collombat P, Mansouri A, Hecksher-Sorensen J, Serup P, Krull J, Gradwohl G, Gruss P. Opposing actions of Arx and Pax4 in endocrine pancreas development. Genes Dev 2003;17:2591–2603
30. Collombat P, Hecksher-Sorensen J, Broccoli V, Krull J, Ponte I, Mundiger T, Smith J, Gruss P, Serup P, Mansouri A. The simultaneous loss of Arx and Pax4 genes promotes a somatostatin-producing cell fate specification at the expense of the α- and β-cell lineages in the mouse endocrine pancreas. Development 2005;132:2969–2980
31. Jensen J, Heller RS, Funder-Nielsen T, Pedersen EE, Lindsell C, Weinmaster G, Madsen OD, Serup P. Independent development of pancreatic α- and β-cells from neurogenin3-expressing precursors: a role for the notch pathway in repression of premature differentiation. Diabetes 2000;49:163–176
32. Hashimoto T, Kawano H, Daikoku S, Shima K, Taniguchi H, Baba S. Transient coappearance of glucagon and insulin in the progenitor cells of the rat pancreatic islets. Anat Embryol (Berl) 1988;178:489–497
33. Herrera PL. Adult insulin- and glucagon-producing cells differentiate from two independent cell lineages. Development 2000;127:2317–2322
34. Gradwohl G, Dierich A, LeMeur M, Guillemot F. Neurogenin3 is required for the development of the four endocrine cell lineages of the pancreas. Proc Natl Acad Sci U S A 2000;97:1607–1611
35. Jensen JN, Rosenberg LC, Hecksher-Sorensen J, Serup P. Mutant neurogenin-3 in congenital malabsorptive diarrhea. N Engl J Med 2007;356:1781–1782
36. Johansson KA, Dursun U, Jordan N, Gu G, Beermann F, Gradwohl G, Grapin-Botton A. Temporal control of neurogenin3 activity in pancreas progenitors reveals competence windows for the generation of different endocrine cell types. Dev Cell 2007;12:457–465
37. Smart NG, Apelqvist AA, Gu X, Harmon EB, Topper JN, MacDonald RJ, Kim SK. Conditional expression of Smad7 in pancreatic β cells disrupts TGF-β signaling and induces reversible diabetes mellitus. PLoS Biol 2006;4:e39
38. Sosa-Pineda B, Chowdhury K, Torres M, Oliver G, Gruss P. The Pax4 gene is essential for differentiation of insulin-producing β cells in the mammalian pancreas. Nature 1997;386:399–402
39. Liew CG, Shah NN, Briston SJ, Shepherd RM, Khoo CP, Dunne MJ, Moore HD, Cosgrove KE, Andrews PW. PAX4 enhances β-cell differentiation of human embryonic stem cells. PLoS ONE 2008;3:e1783
40. Collombat P, Xu X, Ravassard P, Sosa-Pineda B, Dussaud S, Billestrup N, Madsen OD, Serup P, Heimberg H, Mansouri A. The ectopic expression of Pax4 in the mouse pancreas converts progenitor cells into α and subsequently β cells. Cell 2009;138:449–462
41. Schisler JC, Jensen PB, Taylor DG, Becker TC, Knop FK, Takekawa S, German M, Weir GC, Lu D, Mirmira RG, Newgard CB. The Nkx6.1 homeodomain transcription factor suppresses glucagon expression and regulates glucose-stimulated insulin secretion in islet β cells. Proc Natl Acad Sci U S A 2005;102:7297–7302
42. Wilson ME, Kalamaras JA, German MS. Expression pattern of IAPP and prohormone convertase 1/3 reveals a distinctive set of endocrine cells in the embryonic pancreas. Mech Dev 2002;115:171–176
43. Franklin I, Gromada J, Gjinovci A, Theander S, Wollheim CB. β-cell secretory products activate α-cell ATP-dependent potassium channels to inhibit glucagon release. Diabetes 2005;54:1808–1815
44. Banarer S, McGregor VP, Cryer PE. Intraislet hyperinsulinemia prevents the glucagon response to hypoglycemia despite an intact autonomic response. Diabetes 2002;51:958–965
45. Kawamori D, Kurpad AJ, Hu J, Liew CW, Shih JL, Ford EL, Herrera PL, Polonsky KS, McGuinness OP, Kulkarni RN. Insulin signaling in α cells modulates glucagon secretion in vivo. Cell Metab 2009;9:350–361
46. Wideman RD, Covey SD, Webb GC, Drucker DJ, Kieffer TJ. A switch from prohormone convertase (PC)-2 to PC1/3 expression in transplanted α-cells is accompanied by differential processing of proglucagon and improved glucose homeostasis in mice. Diabetes 2007;56:2744–2752
47. Shah P, Vella A, Basu A, Basu R, Schwenk WF, Rizza RA. Lack of suppression of glucagon contributes to postprandial hyperglycemia in subjects with type 2 diabetes mellitus. J Clin Endocrinol Metab 2000;85: 4053–4059
48. Lu J, Herrera PL, Carreira C, Bonnavion R, Seigne C, Calender A, Bertolino P, Zhang CX. α cell-specific Men1 ablation triggers the transdifferentiation of glucagon-expressing cells and insulinoma development. Gastroenterology 2010;138:1954–1965
49. Thorel F, Nepote V, Avril I, Kohno K, Desgraz R, Chera S, Herrera PL. Conversion of adult pancreatic α-cells to β-cells after extreme β-cell loss. Nature 2010;22;464:1149–1154
50. Zhou Q, Brown J, Kanarek A, Rajagopal J, Melton DA. In vivo reprogramming of adult pancreatic exocrine cells to β-cells. Nature 2008;455:627–632